ANALYSIS OF RESIDUAL STRESSES FOR UNDERWATER WET WELDING OF HIGH STRENGTH STEEL

Vasiliy E. Nikulin[1]*, Sergey G. Parshin[1], Alexey M. Levchenko[2], Gennadiy N. Vostretsov[2], Ilia L. Repin[2]

[1]*Institute of Mechanical Engineering, Materials and Transport; Peter the Great St. Petersburg Polytechnic University / St. Petersburg, Russian Federation*

[2]*Department of Underwater Welding and Technologies, Educational Scientific and Technical Center "Svarka" / St. Petersburg, Russian Federation*

*main author, *email:* v.e.nikulin@ya.ru

Introduction

The development of underwater technologies and the exploration of Arctic and Caspian shelves are connected with applying marine metal structures made from high-strength steel. It determines the significance of researches on underwater wet welding [1,2]. Estimation and measuring stress-strain state be of great concern for determining the quality of welded joints high strength steel, especially after underwater welding. The temperature gradient and the rapid cooling rate underwater, stiffness conditions, microstructure heterogeneity, residual welding stresses and hydrogen effusive strongly influence the probability of growth cold cracks in welded joints.

Optimization of a thermal cycle in welding by changing the chemistry of filler material and heat treatment conditions influence reducing residual welding stresses. Therefore, managing retained austenite and martensite formation create a condition for reducing tensile stresses during welding [3]. It induces necessary to assess the stress-strain state welded components. Destructive and non-destructive methods use for measuring, and estimation stress-strain states in metal structures [4,5].

Destructive methods based on cutting, splitting, etching, drilling and electrical discharge machining in materials. The main principle of destructive methods includes measuring deformation by strain gauges and optical systems during or after mechanical machining. In commonly used international practices have been applying the hole-drilling method with using strain gauges according to ASTM E837-13a.

X-ray diffraction method (XRD), among other not-distractive test methods, is widely used for measuring residual stresses in welded components. Use XRD allows estimating the extent of deformation crystal lattice by shifting of diffraction peaks. It is the direct correlation with residual macroscopic stresses. This study considered a compatible way using X-ray diffraction and magnetic anisotropy methods for measuring residual welding stresses in high strength steel after surfacing in air and underwater. The magnetic anisotropy method (MAM) measures electromotive force inducing in detecting coils by an alternating weak magnetic field in ferromagnetic materials. MAM indirectly

correlates with residual shear stresses or the difference between normal stresses for plane stress state [6,7].

Methods of study

This study aimed to determine the residual stresses after surfacing on high-strength steel using different filler materials in air and water environments.

- Preparing samples for calibration MAM measured system;
- Static tensile test of prepared samples for providing calibration MAM results;
- Preparing samples with surfacing by a coated electrode and self-shielded cored wire in air and water environment;
- Measuring and comparing residual welding stresses by MAM and XRD methods.

For research, steel PC D32 thickness of 12 mm was used. The chemical composition of the steel and mechanical properties are given in Tables 1 and 2.

The chemical composition of PC D32 steel, %. Table 1.

C	**Si**	**Mn**	**S**	**P**	**Cr**	**Ni**
0,09	0,22	0,95	0,005	0,013	0,05	0,03
As	**N**	**Al**	**Mo**	**Nb**	**V**	**Cu**
0,003	0,005	0,037	0,005	0,025	0,029	0,06

The mechanical properties of PC D32 steel. Table 2.

Yield point σ_{YP}, MPa	**Ultimate tensile strength** σ_{UTS}, MPa	**Elongation** δ, %	**Elastic modulus** E, MPa	**Poison's ratio** ν
400	490	30	200000	0,29

Tensile test for the calibration

Since the Indicator Mechanical Stresses (IMS) "Stressvision LAB" (Ferrologica LLC, St.Petersburg, Russia) is based on the magnetic anisotropy method, it requires the calibration for used sheet steel PC D32. The sample from this steel was prepared with a dimension of 200x80 mm. The static tensile test has occurred using the "INSTRON 8801" step-by-step from 0 to 30 tonnes-forces, accordingly up to 330 MPa in cross-section of the sample. There are results of calibration in Table 3 and Figure 1. The line of approximation for converting the results of the IMS Stressvision measurement into MPa based on the results of tensile tests can be represented as an equation

$$\sigma = 1{,}287 \cdot \mathrm{SV} + 200 \quad (1),$$

where SV – Mechanical stress in the conditional unit (c.u.). by IMS Stressvision.

Result of calibration IMS "Stressvision LAB". Table 3.

Calculated stresses in cross-section σ_{calc}, MPa	**Imposed force** F, tonne-force	**Result of IMS «Stressvision LAB»** SV, c.u.
0	0	-139
66	6	-120
132	12	-61
198	18	5
264	24	54
330	30	97

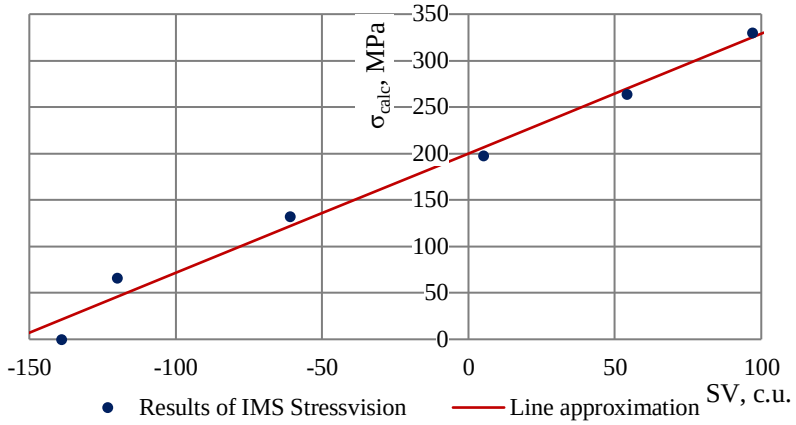

Fig.1. Result of calibration IMS Stressvision during the tensile test for PC D32 steel 15 mm.

Experiments and results

Two samples with dimensions 300x200x12 mm were made from PC D32 steel for surfacing, the same sheet as the sample for the tensile test. The coated electrode for underwater wet welding E38-LKI-1P-3,0-UD (ZAO "Elektrodniy zavod", St.Petersburg) by manual welding and self-shielded cored wire PPS-APL2 (LLC "ESTC "Svarka", St.Petersburg) by automatic welding were used for surfacing in air and water environment. The welding power supply was "Svarog MIG 3500" (LCC "INSVARKOM", St.Petersburg). There are welding parameters in Table 4. When calculating the weld heat input underwater, the efficiency was assumed to be η=0.8 [8]. The calculation of the weld heat input in the welding process was carried out according to the equation:

$$Q = \eta IU/v = \eta P/v \quad (2),$$

Where I – current, A; U – voltage, V; P – arc power W; v – welding speed, m/min.

Welding parameters. Table 4.

Sample	**Filler material**	**Current** I, A	**Voltage** U, V	**Arc power** P, W	**Welding speed** v, m/min	**Weld heat input** Q, kJ/mm
№1 surfacing in air	coated electrode	147	27	3969	0,186	1,07
	self-shielded cored wire	188	32	6016	0,235	1,23
№2 surfacing underwater	coated electrode	141	28	3948	0,186	0,99
	self-shielded cored wire	198	32	6336	0,229	1,32

Measuring residual stresses by magnetic anisotropy method

For measuring residual welding stresses by IMS Stressvision the rectangular grid with coordinates was placed on the surface of samples. Parameters of the grid:

- The numbers of points along axis X are 13;
- The numbers of points along axis Y are 9;
- The step between coordinates are 20 mm;
- The area of measuring 260x180 mm;
- Overall coordinates are 117;
- The seam after surfacing by self-shielded cored wire was placed along 4 line;
- The seam after surfacing by coated electrode was placed along 10 line.

The results of measuring in coordinates are shown as a map of the stress field by parameters difference between σ_y (longitudinal) and σ_x (transverse) stresses or shear stress τ_{yx} according to maximum shear stress theory. Maps of measured stress field taking into account the calibration result (1) are shown in Figure 2. It was noted that the calibration result is an approximate evaluation of the stress state in welding joints without including biaxial residual stresses after weld, influence filler materials and phase transformation.

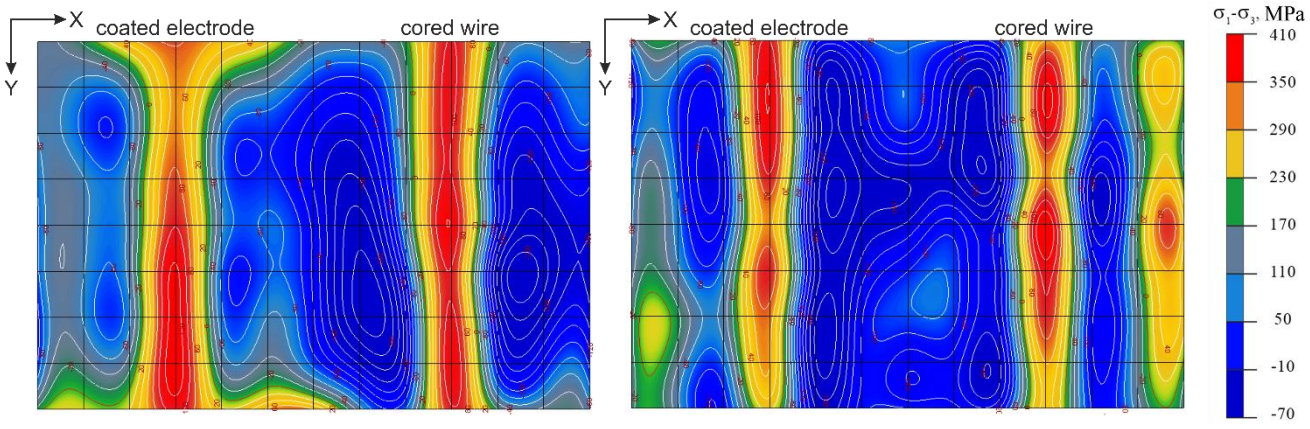

A) B)

Fig.2. Result of measurements residual stresses after surfacing by MAM..
A) Surfacing in air. B) Surfacing underwater.

According to the results of measuring residual stresses for each of the surfacings, the highest values of mechanical stresses in local places in seams was revealed. The magnitude of the high stresses and their location at these coordinates are shown in Table 5. Subsequent use of X-ray diffraction was carried out at these coordinates on the seam and in the area of HAZ and the base metal.

Maximum of residual stress by MAM results. Table 5.

Filler material and environment	self-shielded cored wire in air	self-shielded cored wire underwater	coated electrode in air	coated electrode undewater

σ_y-σ_x, MPa	370	353	352	376
coordinates on the seam X;Y	4;8	4;2	10;5	10;5

Measuring residual stresses by X-ray diffraction method

The device "NeRKA" (LLC "Radiatech", Gatchina) was used for the X-ray diffraction method. The device includes two chrome anodes that provide shooting at two angles $\psi_1 = 0^o$ and $\psi_2 = 38^o$. This device allows measuring residual stresses in the direction of shooting to determine the displacement of diffraction peaks after X-ray radiation is reflected from the surface plane (211) for α-Fe. The diameter of the X-ray beam for two anodes is 2 mm. Bragg's law describes diffraction from elastic X-ray scattering on a crystal:

$$2d_{hkl} \sin\theta = n\lambda \quad (3),$$

where d_{hkl} – inter-planar spacing, Å; θ – angular position of the diffraction lines according to Bragg's Law; n – an integer, $n = 1$; λ – wavelength of the X-ray, for chrome anode $\lambda_{CrK\alpha} = 2{,}2897$ Å.

The calibration of "NeRKA" provides analysis diffraction peaks on the powder of iron. An example of diffraction peaks for carbonyl iron powder is shown in Figure 3.

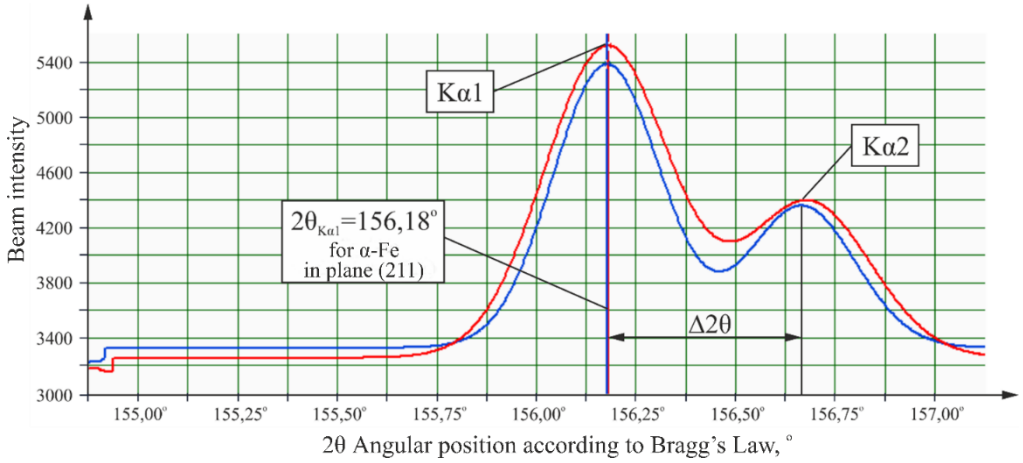

Fig.3. Diffraction peaks for carbonyl iron.

The diffraction peaks shown blue in Figure 3 are obtained from the X-ray beam incident at an angle of 90° to the surface of the powder ψ_1=0°. Diffraction red peaks are obtained from an X-ray beam incident at an angle of 52° to the surface of the powder ψ_2=38°. The Ka1 transition is located at the diffraction angle $2\theta_1$=156,18°, the distance between energy transitions was $\Delta 2\theta$=0,94°, which corresponds to the location of the diffraction peaks for the (211) α-Fe plane, according to the COD (crystallography open database), PDF-2 (Powder Diffraction File).

The separation of the signal into two energy transitions characterizes mechanical uniformity for microscopic stresses and the absence of micro-damage to the crystal lattice. The coincidence of the diffraction peaks obtained when X-ray radiation falls on the crystal plane at two different angles indicates zero macroscopic stresses and the absence of deformations of the crystal lattice.

For example, a result of measure residual stress for the seam after underwater wet surfacing self-shielded cored wire in the coordinate 4;8 (Table 5) is shown in Figure 4. All results of measured stresses by XRD are shown in Figure 5, maximum residual stresses in seams after surfacing are put in table 6.

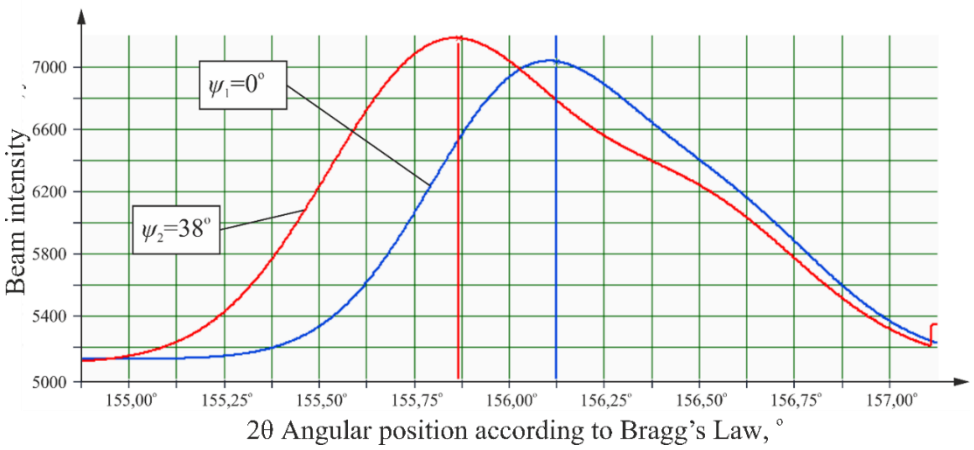

Figure 4. Diffraction peaks for the seam in longitudinal direction after underwater wet surfacing self-shielded cored wire.

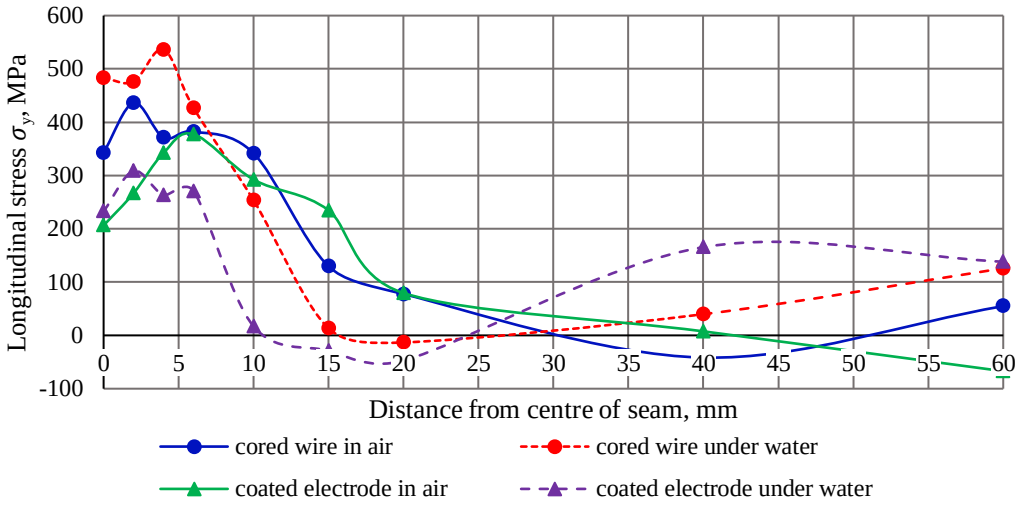

A)

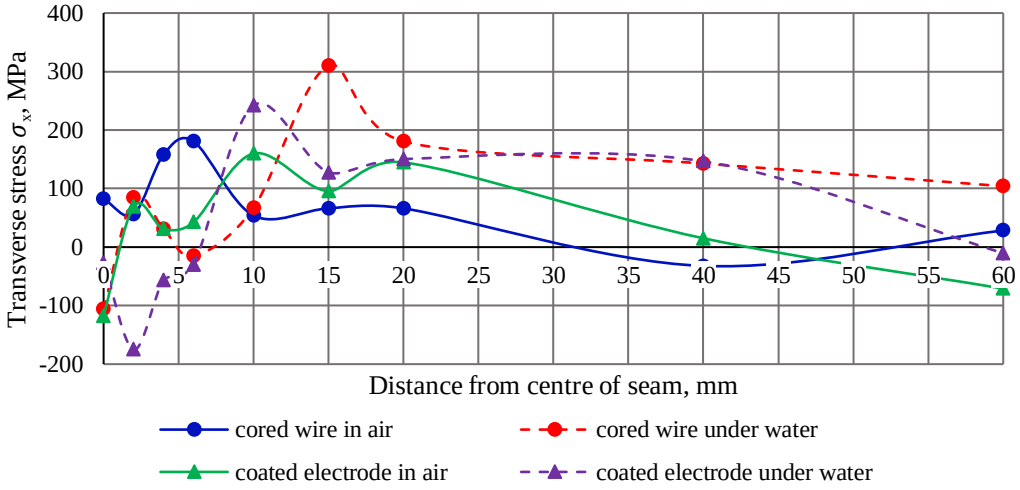

B)

Figure 5. Result of measurements residual stresses after surfacing by XRD. A) Longitudinal stress σ_y; B) Transverse stress σ_x.

Maximum residual stresses by XRD results. Table 6.

Filler material and environment	self-shielded cored wire in air	self-shielded cored wire underwater	coated electrode in air	coated electrode undewater
Longitudinal stress σ_y, MPa	438	536	378	308
Transverse stress σ_x, MPa	181	310	160	242

Comparing results of measuring residual stresses

The assessment of residual stresses by two different physical methods does not allow to carry out measurements with absolute accuracy [9]. The comparison of the measurement results includes both advantages and disadvantages of described methods. MAM allows to fast results of stress field map in a short time without preparing and cleaning the surface, but it requires calibration in static test, and biaxial stress components require a more in-depth analysis. The XRD method makes it possible to measure normal stresses with high accuracy, but such measurements require much more time and more careful surface preparation. Comparative results of measuring residual stress by MAM and XRD on the parameters of the difference between longitudinal and transverse mechanical stresses are shown in Figure 6.

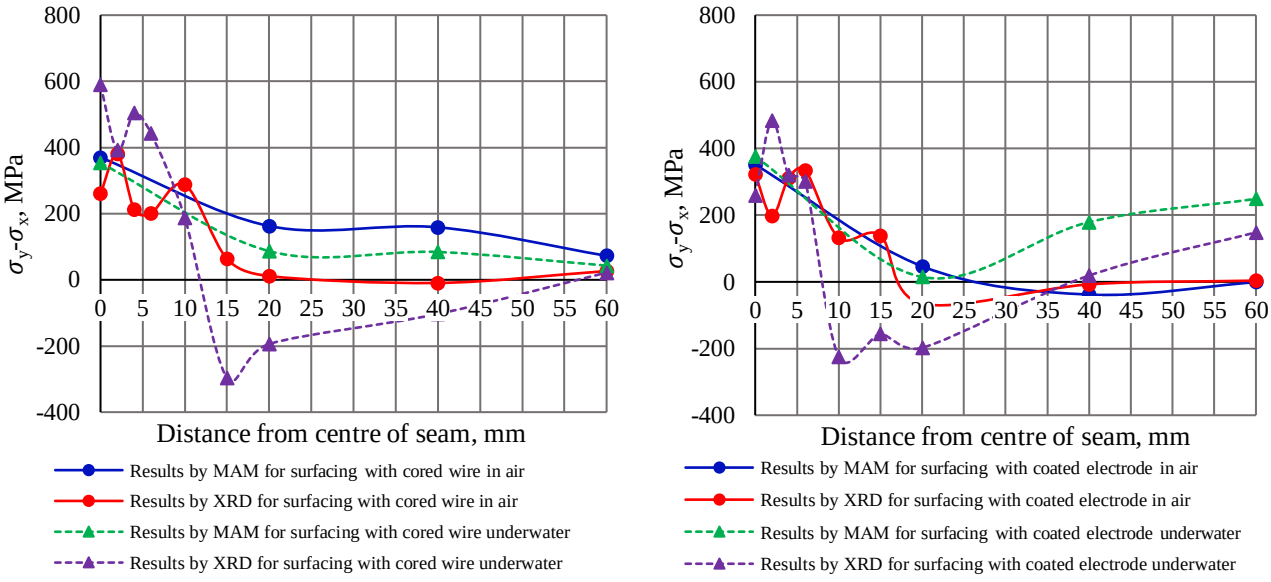

A) B)

Fig.6. Comparative results of measuring residual stress by MAM and XRD in samples with surfacing in air and underwater environment. A) Surfacing with cored wire. B) Surfacing with the coated electrode.

Conclusion

The use of XRD and MAM made it possible to determine the magnitude and distribution of residual stresses in high-strength steel after surfacing. For underwater wet welding of high-strength steel, the high heat input and cooling rate increase the residual stresses in HAZ and the welded seam up to 578 MPa. To prevent the formation of cold cracks during underwater wet welding is necessary to reduce residual stresses by using heat treatment or vibration treatment of welded joints, increasing the plasticity of the deposited metal.

References

1. Parshin S.G. Metallurgija podvodnoji giperbaricheskoj svarki [Metallurgy underwater and hyperbaric welding]. SPb.: Izd-vo Politehn. Un-ta, 2016. 402 p.
2. Parshin S., Levchenko A. Technology and equipment for underwater wet welding and cutting of high strength steel arctic structures using flux-cored wires. IOP Conference Series: Earth and Environmental Science. 2020. No 539. P. 1–10.
3. Karkhon V.A. Teplovie processi pri svarke [Thermal processes during welding]. SPb.: Izd-vo Politehn. Un-ta, 2015. 402 p.
4. Rossini N.S., Dassisti M., Benyounis K.Y., Olabi A.G. Methods of measuring residual stresses in components // Materials and Design. 2012. V. 35. P. 572—588.
5. Schajer G.S. Practical Residual Stress Measurement Methods, First Edition. John Wiley & Sons, Ltd. Published, 2013. 297 p.
6. Mogil’ner L.Yu., Skuridin N.N. Laboratornye issledovaniya magnitno-anizotropnogo metoda kontrolya napryazhenno-deformirovannogo sostoyaniya truboprovodov [Laboratory studies of the magnetoanisotropic method for monitoring the stress-strain state of pipelines] // Nauka i tekhnologii truboprovodnogo transporta, nefti i nefteproduktov. 2021. № 11(2). 145–151 pp.
7. Zhukov S.V., ZHukov V.S., Kopica N.N. Sposob opredeleniya me-hanicheskih napryazhenij i ustrojstvo dlya ego osushchestvleniya [The method for determining mechanical stresses and a device for its implementation] // Patent of the Russian Federation № 2195636. 2001
8. Yong Zhang, Chuanbao Jia, Bo Zhao and et al. Heat input and metal transfer influences on the weld geometry and microstructure during underwater wet FCAW // Journal of Materials Processing Technology. 2016, V. 238. P. 373–382.
9. Gurova T., Estefen S.F., Leontiev A. Time-dependent redistribution behavior of residual stress after repair welding // Welding in the World. 2017, V. 61. P. 507–515.